Case Studies in Fire Safety 5 (2016) 34–41

Contents lists available at ScienceDirect

Case Studies in Fire Safety

journal homepage: www.elsevier.com/locate/csfs

Assessing the influence of fuel geometrical shape on fire dynamics simulator (FDS) predictions for a large-scale heavy goods vehicle tunnel fire experiment

Xiaoyun Wang*, Charles Fleischmann, Michael Spearpoint

Civil and Natural Resources Engineering, University of Canterbury, Christchurch, New Zealand

ARTICLE INFO

Article history:
Received 20 November 2015
Received in revised form 7 April 2016
Accepted 7 April 2016
Available online 29 April 2016

Keyword:
Tunnel fires
HGV
FDS
Fuel geometrical shape

ABSTRACT

This paper uses four different simple geometrical shapes to simulate a large-scale heavy goods vehicle (HGV) tunnel fire experiment using Fire Dynamics Simulator, version 6 (FDS6) in order to investigate the influence of using different fuel package shapes. Simulations also investigate the influence on temperature profiles when a large target is placed downstream of the fuel package. Predictions of flame extension, temperature profiles and gas species concentrations are compared with the experimental data. The use of the geometrical shapes causes significant differences in flame extension lengths during the fully developed fire phase. The variation in temperature predictions caused by using the different fuel shapes are insignificant when a large target is present behind the fire, however this is not the case if the target is omitted especially during the fully developed phase.

1. Introduction

Fires in tunnels are often caused by vehicle accidents that occur inside them. The characteristics of the fire depend on the various types of vehicles involved and for road tunnels these could include passenger cars, utility vehicles, buses and/or heavy goods vehicles (HGVs). HGVs usually have much larger dimensions and carry goods that can cause more severe fires than normal passenger cars. Therefore HGV fires can pose a greater risk to life safety and property protection than fires caused by other types of vehicles.

Fire Dynamics Simulator version 6.2.0 (FDS6) [1] is a commonly used tool in fire engineering to simulate fires. In FDS, a typical way to simulate a given heat release rate (HRR) fire is to represent it as the ejection of gaseous fuel from a solid surface by a 2D 'gas burner'. In previous work Li et al. [2] used a simple 2D gas burner with a dimension of 3 m × 10 m to represent the HGV to simulate the Runehamar tunnel fire experiment using FDS. This 2D gas burner representation of a fire is also specified in the New Zealand Verification Method: Framework for Fire Safety Design [3]. The results in the study of Li et al. showed that the simplified 2D gas burner of HGV could give reliable predictions of ceiling temperatures along the tunnel length however, Li et al. did not predict temperature profiles at different tunnel cross section locations. In the work of Cheong et al. [4] a more complex fuel representation was used to simulate the Runehamar HGV fire experiment where the fuel package surface area in the simulation was equivalent to the fuel surface area in the experiment and the inputted HRR curves were based on cone

* Corresponding author.
E-mail address: xiaoyun.wang@pg.canterbury.ac.nz (X. Wang).

http://dx.doi.org/10.1016/j.csfs.2016.04.001

calorimeter experimental results. The approach used in their work was mainly for the prediction of HRR of tunnel fires using FDS and the influence on temperature distributions due to the geometrical shape of the HGV was not investigated in their work.

For an HGV fire that occurs under a forced ventilation condition, the burning behaviour will be affected by the airflow [5,6]. The physical dimensions of the HGV will also interact with the airflow so that the behaviour of the fire and the downstream temperature distribution in the tunnel will likely be further affected. Any changes in the shape of the fuel package due to material burning away or the collapse of the fuel package will result in additional effects on the fire and hence the temperature distributions. Therefore, it is important to take into account the large geometrical vehicle shape in the simulations of HGV fires.

In this case study, a series of simulations are carried out to model a large-scale HGV tunnel fire experiment by using different simple geometrical shapes to represent the HGV in order to investigate the influence of the shape of fuel package on flame extensions, the distributions of temperature and gas concentrations. Several simplifications have been made in order to carry out the simulations in a practical manner.

2. The LTA tunnel fire experiment

A series of large-scale HGV tunnel fire experiments [7] were conducted on behalf of the Land Transport Authority (LTA) of Singapore in a tunnel test facility in Spain. A rectangular shape test section was used for all the experiments, which had a minimum cross section of 7.3 m (W) × 5.2 m (H) and 1% longitudinal gradient. The length of the test tunnel was 600 m and the fire was located 350 m away from the south portal. Measurement points in the tunnel were installed from 30 m away from the upstream edge of the fire to 170 m away from the downstream edge of the fire.

The tunnel section in which the measurements were made is shown in Fig. 1 together with the instrumentation locations. Temperatures were measured using thermocouples at the different cross sections shown in Fig. 1(a) and gas concentrations of O_2, CO_2 and CO were measured at location D170. The cross sections with the thermocouple locations at D10, D15 and D30 are illustrated in Fig. 1(b).

The fuel source consisted of 228 pallets with 48 plastic pallets (20% by volume) and 180 wood pallets (80% by volume) [8], in a configuration representative of a fully loaded HGV (7.5 m (L) × 2 m (W) × 3 m (H)). According to the averaged densities of the plastic (1376 kg/m^3) and wood (566 kg/m^3) from the LTA, the estimated mass fractions of plastic and wood pallets are ~38% and 62%, respectively. The fuel source was elevated 1 m above floor and in addition, the top side, the front side and the back side of the fuel source were covered by steel plates to represent a typical HGV configuration. During the experiment the fuel source collapsed as the pallets burned away.

In addition to the fuel source, a target consisting of a stack of pallets with dimension of 1.2 m (L) × 2 m (W) × 3 m (H) was used in the experiments that was located 5 m from the downstream edge of the fuel source.

Jet fans at the southern end of the tunnel were used to generate longitudinal air flow with a desired velocity of 3 m/s in all of the experiments. According to the measurements [7] at the upstream side of the fire, an average of 3 m/s was maintained in the upper cross section of the tunnel, while lower velocities were obtained in the lower cross section. A total of seven experiments were conducted, six with a water suppression system in the vicinity of the HGV and one without. In this study,

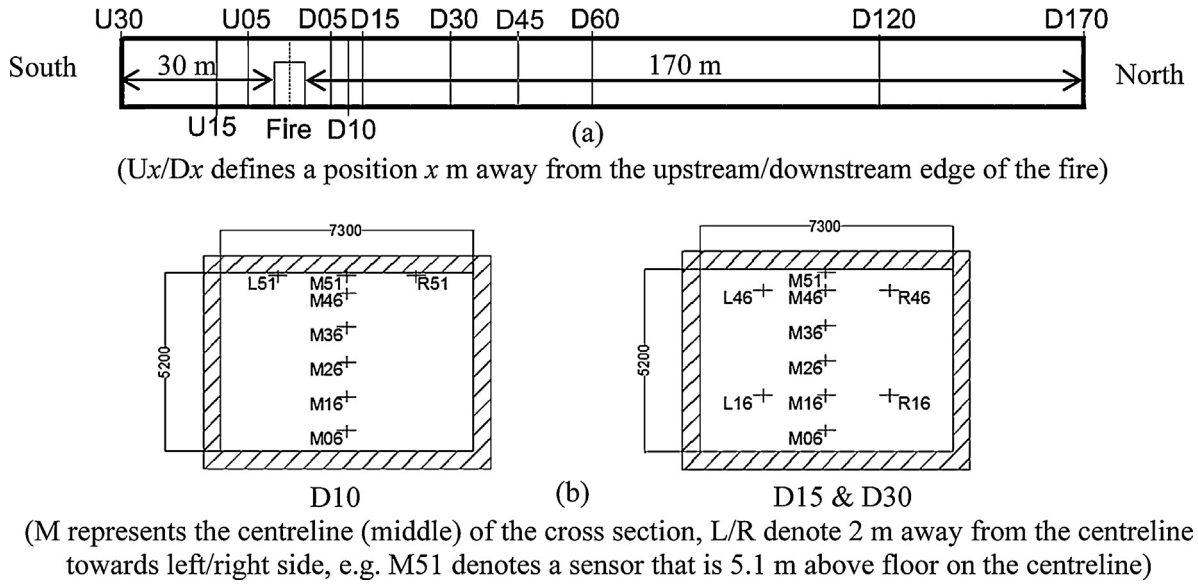

Fig. 1. (a) Tunnel with the measurement locations, (b) tunnel cross sections.

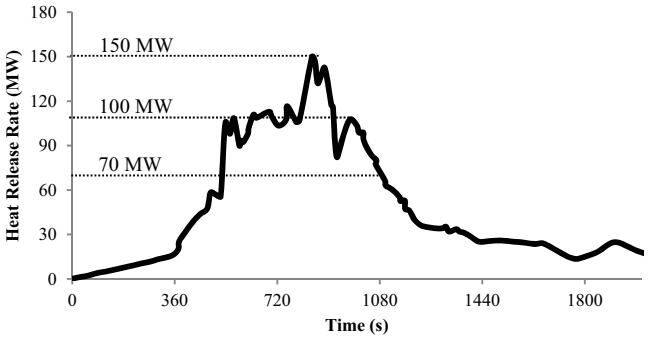

Fig. 2. HRR curve in the large-scale experiment, adapted from [7].

only the results without the operation of water suppression system are used. The corresponding HRR curve is shown in Fig. 2. According to the information provided by the LTA, water spray was used to cool down the tunnel structure at the D45 location 9 min after ignition. However, the water discharge had no influence on the temperature results recorded at locations of D10, D15 and D30 and no influence on the burning and hence the HRR of the HGV (measured O_2, CO_2 and CO concentrations).

3. FDS simulation set-up

3.1. Tunnel geometry and basic settings

As indicated in Fig. 1, the test section had dimensions of 7.3 m (W) × 5.2 m (H) × 210.5 m (L). In order to minimise any influence on the simulation results of sudden changes in temperature at the open ends, the tunnel section in FDS is extended to 240 m including 35 m upstream and 205 m downstream from the centre of the fire. Walls, ceiling and floor are defined as concrete having thermal conductivity of 1.2 W/m.K, specific heat of 0.88 kJ/kg.K and density of 2000 kg/m^3 [9]. A radiative fraction of 35% is used as a reasonable estimate in this work. The 1% longitudinal gradient is modelled through the gravitational vector (GVEC) function in FDS6. Thermocouple devices are set up at the D10, D15 and D30 locations to correspond with the measurement locations in Fig. 1(b). Thermocouple devices were not included at the D45 location or further downstream because of the influence of the water spray. In addition, the concentrations of O_2, CO_2 and CO are determined at the D170 location.

In order to simulate the experiment several simplifications are made. A 3D solid block with adjusted dimension of 1.2 m (L) × 2.19 m (W) × 3.12 m (H) based the grid resolution is used to represent the target stack of pallets, however, the porous nature of the pallet stack is not modelled as a much finer subgrid size is needed, which is beyond the scope of this work. A uniform velocity of 3 m/s is applied to a solid surface at the upstream end of the tunnel blowing air towards the tunnel to represent the forced ventilation condition and the downstream boundary condition is specified as ambient. The complexity of simulating the measured velocity profile is not attempted in this work.

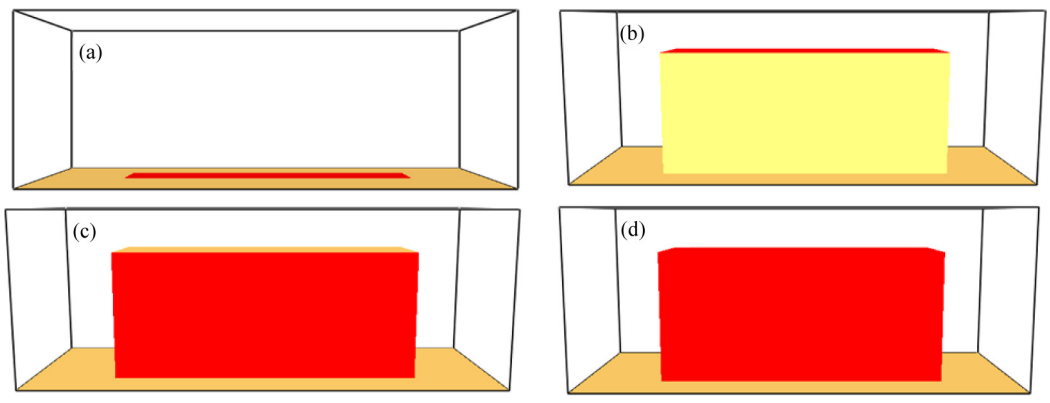

Fig. 3. Different gas burner surface arrangements: (a) Scenario 2DF; (b) Scenario 2DT; (c) Scenario 3DS; (d) Scenario 3DA;.

Table 1
Relationship between D^* and $\delta x, \delta y, \delta z$ for different fire heat release rates and different cell sizes.

$\delta x, \delta y, \delta z / D^*$		150 MW	100 MW	70 MW
		D^* (7 m)	D^* (5.9 m)	D^* (5.2 m)
δx	30 cm	$0.043D^*$	$0.034D^*$	$0.058D^*$
δy	36.5 cm	$0.052D^*$	$0.062D^*$	$0.070D^*$
δz	26 cm	$0.037D^*$	$0.044D^*$	$0.050D^*$

3.2. Fuel source

The four different fuel package shapes shown in Fig. 3 are used to represent the HGV fire. The 2DF scenario simplifies the HGV fire to a 2D gas burner on the tunnel floor; in scenario 2DT a 3D solid block is used to represent the HGV and the gas burner is set up on the top surface of the solid block; scenario 3DS mimics the actual fuel source arrangement in the experiment, where the top, upstream, and downstream surfaces of the HGV were covered by the steel plates such that a 3D solid block is used with only the longitudinal surfaces of the block assigned as the gas burners. Scenario 3DA uses the top and all four vertical surfaces but not the bottom surface of a 3D block to simulate the HGV fuel package. To simplify the modelling no attempt is made to simulate the collapse of the fuel source during the experiment.

In order to describe the gas phase combustion reaction, the 'simple chemistry' [1] approach is used. The chemical formula in the simulations is specified as $CH_2O_{0.62}$ which combines values for 38% plastic $(CH_2)_n$ [10] and 62% wood $(CH_2O)_n$ [9]. The yields of CO (y_{co}) and soot (y_s) are defined as 0.012 g/g and 0.012 g/g, respectively which are derived from combining 38% y_{co} and y_s yields for plastic and 62% y_{co} and y_s yields for wood [10]. The combined heat of combustion for the fuel is 20 MJ/kg based on the information provided by the LTA.

3.3. Grid size

According to the FDS6 user's guide [1], the quantity $D^*/\delta x$ represents the number of computational cells spanning the characteristic diameter of the fire, where δx is the nominal size of a mesh cell and D^* is a characteristic fire diameter defined through the HRR of a fire and the thermal properties of ambient conditions. In general the more cells spanning the fire, the better resolution in the simulation.

In the work of Li et al. [2] $0.075D^*$ was shown to be a reasonable value to determine the cell size and a 20 cm uniform cell size was used to simulate Runehamar tunnel Test 1, where the maximum HRR was 202 MW. Cheong et al. recommended 30 cm mesh size in their FDS simulations of the Runehamar tunnel experiment [4].

With consideration of the numerical accuracy, the computational time and the actual tunnel dimensions, a rectangular mesh size is proposed in all of the simulations in this work, which is less than $0.075D^*$ in the x, y and z directions. Table 1 lists the relationships between D^* and $\delta x, \delta y, \delta z$ when different fire heat release rates are applied (where $\delta x, \delta y$ and δz are the cell sizes in the x,y and z directions). The cell sizes in Table 1 are determined from the length, width and height of the tunnel to ensure that there are an integral number of cells in each direction. Three different heat release rates (150 MW, 100 MW and 70 MW) from the curve shown in Fig. 2 are used to calculate characteristic diameter of the fire to correspond to the instantaneous peak, 'average' maximum steady state and value during the growth and decay phases.

Based on the cell sizes for the x, y and z directions given in Table 1, the dimensions of the experimental fuel package (7.5 m (L) × 2 m (W) × 3 m (H)) are adjusted to obtain an integral number of cells for the four different geometrical fuel shape scenarios as shown in Table 2. The FDS RAMP_Q function is adopted to specify the heat release rate curve (Fig. 2). As different fuel surface areas are used in the four different scenarios, the values of heat release rate per unit area (HRRPUA) are different as shown in Table 2. The FDS HRR results based on different scenarios are verified, which all match to the experimental HRR curve.

Table 2
Fuel dimensions and HRRPUA in different fuel geometrical shape scenarios.

Scenario	Fuel dimensions	HRRPUA (kW/m^2)
2DF	7.5 m (L) × 2.19 m (W)	9140
2DT	7.5 m (L) × 2.19 m (W)	9140
3DS	7.5 m (L) × 2.19 m (W) × 3.12 m (H)	3205
3DA	7.5 m (L) × 2.19 m (W) × 3.12 m (H)	1949

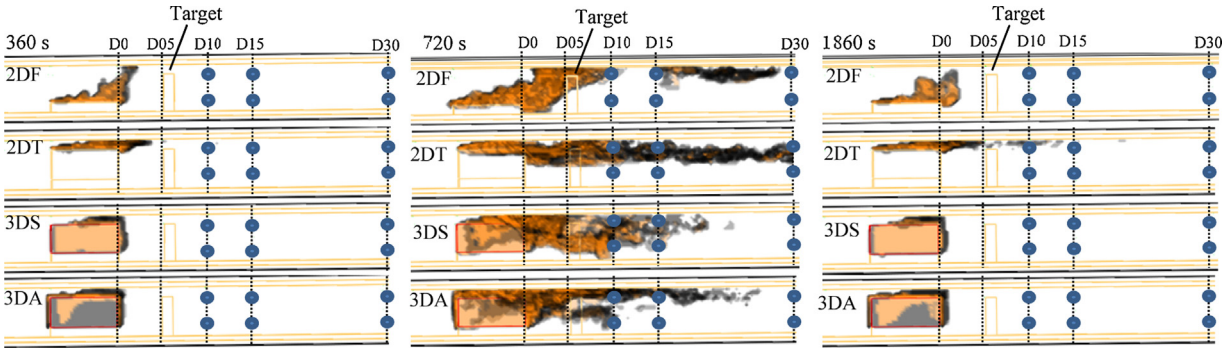

Fig. 4. Flame extension images at different fire development stages for the four scenarios.

4. Results and discussion

4.1. Flame extension

The FDS6 output quantity 'HRRPUV' is rendered through Smokeview to provide a means to visualise the flame boundary. Fig. 4 shows the predicted flame extension for the four different fuel package geometrical shapes at 360 s, 720 s and 1860s, which represent burning behaviour during the initial fire growth phase, fully developed phase and the decay phase.

Flame extension lengths are determined from FDS over the time periods 345–375 s, 705–735 s and 1845 to 1875s, to correspond to the initial fire growth, fully developed and decay phases respectively. The flame length is defined as the

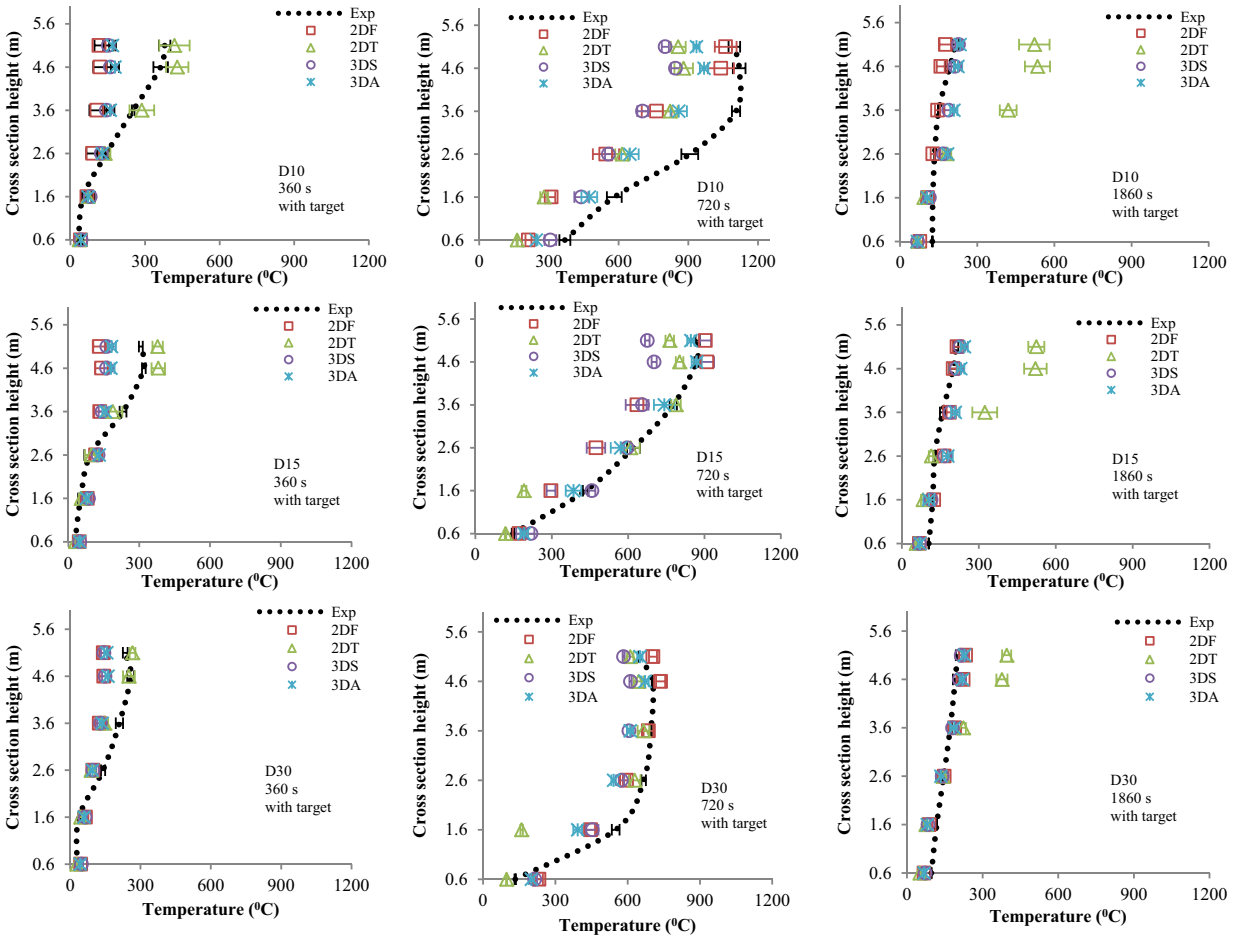

Fig. 5. Temperature results at different fire development stages for the four scenarios with the downstream target.

horizontal flame length, where is the distance from the impingement point of the fire source centre to the flame tip [11]. The overall predictions for flame length during the initial fire growth phase and the decay phase are similar such that there is no obvious flame extension beyond the fuel burning surface area. The significant differences in the predictions of flame extension mainly occur during the fully developed fire phase. In the 2DF scenario the flame extends along the floor to a downstream location 14 m away the fuel centre. In the 2DT scenario the flame extends to more than 30 m away from the fuel centre location. In scenario 3DS and scenario 3DA, the entire 3D block is surrounded by the fire and the flame length extends to ~25 to 30 m on the downstream side.

According to the equation in Tunnel Fire Dynamics [11], the flame length of an HGV fire can be predicted from:

$$L_f = 5.5HQ_f^* \tag{1}$$

where L_f is the horizontal flame length, H is the tunnel height and Q_f^* is dimensionless heat release rate. Based on the HRR curve in Fig. 2, the $\dot{Q}$ values at the initial fire growth phase, fully developed phase and decay phase are 20 MW, 100 MW and 20 MW, respectively and therefore, the corresponding L_f is calculated as 6 m, 33 m and 6 m. Comparing the results obtained from this mathematical model with the predictions from FDS, it is found that Equation (1) gives values close to the FDS6 predictions for the 3DS and 3DA scenarios in the fully developed fire phase. However, since the actual flame length in the experiment was not recorded it is not possible to verify whether the predicted values match reality.

4.2. Gas temperature

The corresponding predicted temperature results for the three different fire development phases at the D10, D15 and D30 cross sections are shown in Fig. 5 along with the experimental temperature results. The plotted temperatures at 360 s 720 s and 1860s are average and standard deviation values for the time periods 345–375 s, 705–735 s and 1845 to 1875s, respectively.

As shown in Fig. 5, during the initial fire development phase, scenario 2DT gives the most effective temperature predictions at the D10, D15 and D30 cross sections. The temperature results for the other scenarios at the upper locations are all slightly underpredicted. During the fully developed phase the predicted temperatures for the four scenarios can all represent the temperature gradients in the experiment at the different cross sections. In particular, the predictions at locations D15 and D30 are closer to the experimental results than the predictions at location D10. The temperature results at D10 are all underpredicted. During the decay phase the results from scenarios 2DF, 3DS and 3DA are all similar, and all match with the experimental temperature curves at the different cross sections. Scenario 2DF may physically demonstrate the actual fuel geometrical shape due to the collapse of the fuel package in the decay phase, while the difference in temperature profiles based on the three scenarios is negligible. The results from scenario 2DT have much higher temperature values at the upper locations for the different cross sections suggesting the set-up of a gas burner on a 3D block top surface does not represent the temperature profiles due to the collapse of the fuel package in decay phase.

Overall, the results in Fig. 5 shows that when the target obstacle is present on the downstream side of the fire, the different fuel geometrical shapes only weakly affect the temperature distributions downstream of the obstacle. It is interesting to compare the simulation results for the situation in which the target behind the fire is removed. Fig. 6 illustrates the temperature predictions at D10, D15 and D30 cross sections without the presence of the target in the simulations. In order to compare with the results in Fig. 5, the experimental temperature profiles are also plotted.

As seen in Fig. 6, the predicted temperature distributions during the initial fire growth phase and the fire decay phase are similar to those shown in Fig. 5. However, the predicted temperatures for the four scenarios show distinct differences during the fully developed phase and of the four scenarios it appears that 3DA gives the closet match with the experimental results.

4.3. Gas species concentration

In FDS, the predictions of gas species (O_2, CO_2 and CO) are determined by the chemical formula and the given values of y_{co} in the input file. In this study, the chemical formula of the fuel and y_{co} are estimated based on the previously discussed mass fractions of plastic and wood pallets. In the experiment, the concentrations of O_2, CO_2 and CO were measured at location D170. Since the different fuel geometrical shapes result in different flame extension behaviour and different temperature distributions it is also instructive to observe the influence on the gas concentration predictions. Fig. 7 presents the comparisons for the concentrations of O_2, CO_2 and CO between the simulation results from the four different fuel shape scenarios and the experimental results. A moving average technique is used to smooth the curves for the FDS6 predictions.

As shown in Fig. 7, different concentration predictions of O_2, CO_2 and CO are obtained in scenario 2DT compared with the predictions from the other three scenarios. The negligible differences in gas concentrations based on scenarios 2DF, 3DS and 3DA suggests that the predicted gas species are sufficiently mixed at the downstream D170 location and are not affected by the three different geometrical shapes. However, when the scenario 2DT is applied, the different gas concentrations profiles shown in Fig. 7 indicate that the 2DT geometrical shape considerably affects the gas species distributions even when the location is 170 m away from the fire.

Comparing the predicted concentrations of O_2, CO_2 and CO from the scenarios 2DF, 3DS and 3DA to the experimental concentration curves, the predicted O_2 and CO_2 concentration curves are close to the experimental curves, while the

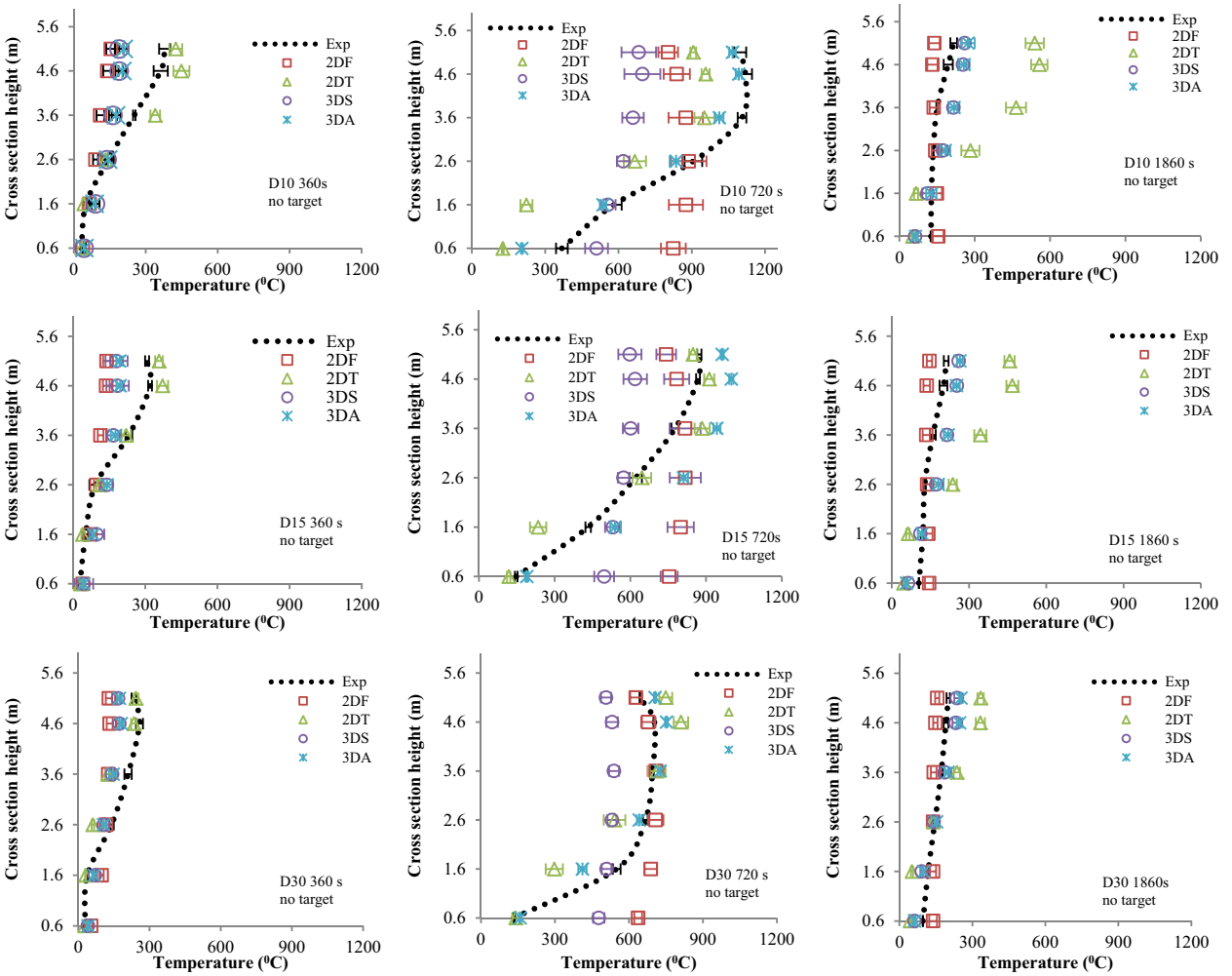

Fig. 6. Temperature results at different fire development stages for the four scenarios without the downstream target.

concentration curve of CO is significantly overpredicted. The results suggest that the values of O and C based on mass fractions of plastic and wood pallets can give adequately accurate predictions in FDS6. However, the value of 0.012 g/g CO yield in the simulations is higher than the CO yield in the experiments, which results overpredicted CO concentration values.

Overall, the predictions in Fig. 7 can effectively demonstrate the changes in the concentrations of O_2, CO_2 and CO with the development of fire. However, the species measurements should be viewed caution due to the unknown quantity of water vapour included in the combustion products from the water spray which has not been included in the simulations.

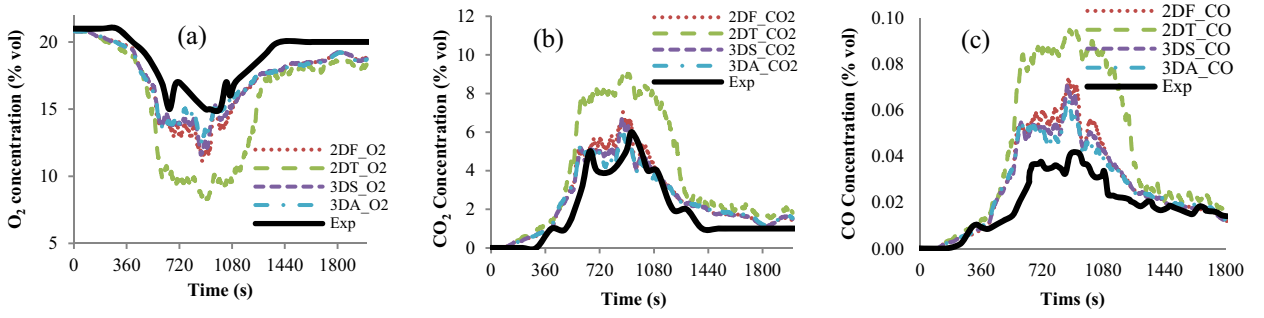

Fig. 7. Predictions of gas concentrations (a) O_2, (b) CO_2, (c) CO.

5. Conclusions

This work uses four different simplified geometrical shapes in FDS6 to simulate a fuel package that represents a large-scale HGV tunnel fire which includes the influence of a forced ventilation system. It is found that flame extension predictions are affected by the use of fuel geometrical shapes when the fire is fully developed. During this phase the predicted values of flame length (~25 to 30 m) in scenarios in which vertical as well as horizontal surfaces are burning (3DS and 3DA) are similar to the values calculated from the Ingason et al's model. The use of the different geometrical shapes only weakly affects the predicted temperature distributions in the presence of the large target located downstream of the fire. However significant differences are obtained during the fully developed phase using the different fuel shapes without the presence of the target. Finally the 2D burner on the top of the fuel package scenario (2DT) results in different predicted gas distribution profiles at location D170 when compared with the three other geometrical scenarios.

In summary this case study highlights the influence of using different fuel geometrical shapes on flame extension, temperature distributions and gas species concentrations during different fire development phases. Depending on the objective the results from this work suggest that the use of 'a 2D gas burner' in fire engineering simulations using FDS may not always be suitable in cases involving a fuel package that creates a blockage within a tunnel that is subject to a forced ventilation. The work also illustrates the potential importance of including any large target items that are located downstream of the fire.

Acknowledgements

The primary author gratefully acknowledges the University of Canterbury, New Zealand for the UC Doctoral Scholarship award; Dr. Mun Kit Cheong from the Land Transport Authority, Singapore for the providing the large-scale tunnel experimental data used in this work.

References

[1] K. McGrattan, R. McDermott, S. Hostikka, J. Floyd, NIST Special Publication 1019 Fire Dynamics Simulator User's Guide Version 6, National Institute of Standards and Technology, 2015.
[2] Y.Z. Li, H. Ingason, Numerical simulation of runehamar tunnel fire tests, 6th International Conference 'Tunnel Safety and Ventilation', Graz, 2012, pp. 203–210.
[3] Verification Method: Framework for Fire Safety Design. 2014, Ministry of Business Innovation & Employment: Wellington New Zealand
[4] M.K. Cheong, C.M. Fleischmann, M.J. Spearpoint, Calibrating an FDS Simulation of Goods-vehicle Fire Growth in a Tunnel Using the Runehamar Experiment (2009).
[6] H. Ingason, Fire dynamics in tunnels, The Handbook of Tunnel Fire Safety, second edition, Thomas Telford, London, 2012.
[7] M.K. Cheong, W.O. Cheong, K.W. Leong, A.D. Lemaire, L.M. Noordijk, Heat release rate of heavy goods vehicle fire in tunnels with fixed water based fire-Fighting system, Fire Technol. 50 (2) (2014) 249–266.
[8] M.K. Cheong, W.O. Cheong, K.W. Leong, A.D. Lemaire, L.M. Noordijk, F. Tarada, Heat release rate of heavy goods vehicle fires in tunnels, 15th International Symposium on Aerodynamics, Ventilation& Fire in Tunnels, Barcelona, Spain, 2013.
[9] D. Drysdale, An Introduction to Fire Dynamics, second edition, Wiley, Hoboken, N.J, 2011.
[10] A. Tewarson, Generation of heat and chemical compounds in fires, SFPE Handbook of Fire Protection Engineering, third edition, National Fire Protection Association, 2002.
[11] H. Ingason, Y.Z. Li, A. Lönnermark, SpringerLink, H. Mälardalens, E. Framtidens, Akademin för ekonomi s.o.t, Tunnel Fire Dynamics, 2015, Springer New York, New York, NY, 2015.